Biogeosciences

Open Access

EGU

Supplement of

Spatial and temporal variability of methane emissions and environmental conditions in a hyper-eutrophic fishpond

Petr Znachor et al.

Correspondence to: Anna Matoušů (anna.matousu@gmail.com)

Figure S1. Aerial view of the Dehtář fishpond from the west.

Figure S2. Bubbles of gases (ebullition) accumulated on the water surface, August 14, 9:00.

Figure S3. Dense zooplankton "clouds" accumulating at the surface near the dam due to the severe oxygen depletion in the deeper strata of the water column, August 14, 9:00.
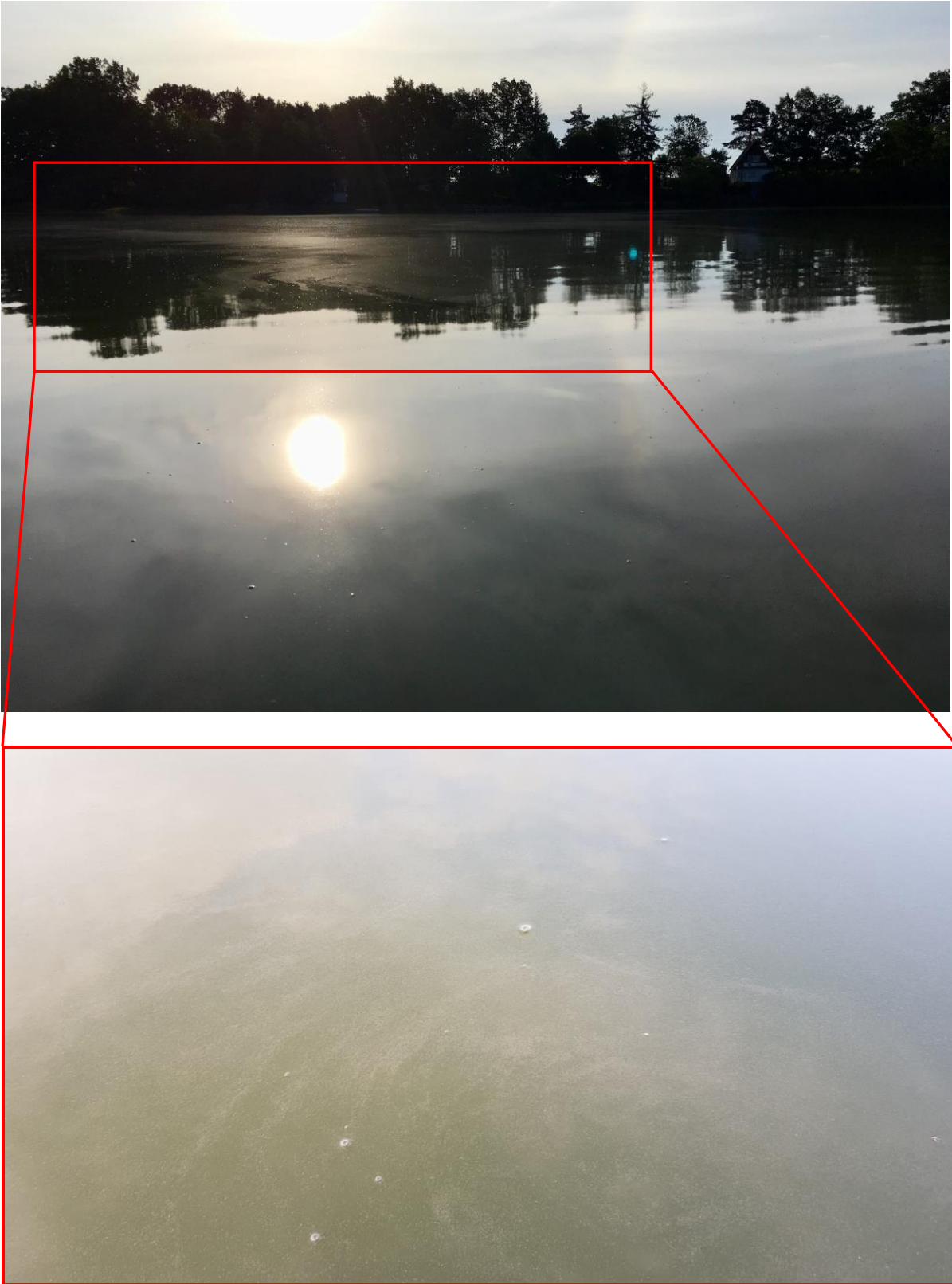
Figure S4. North-south transects of the temperature (A, C, E; °C) and chlorophyll-a concentration (B, D, F; µg L^{-1}). Panels A and B are morning, C and D evening and E and F next-morning measurements. A grey area is a bottom. The right insert is a map of the Dehtář fishpond (credit Jiří Jarošík) with red points 1–6 indicating the sampling sites.
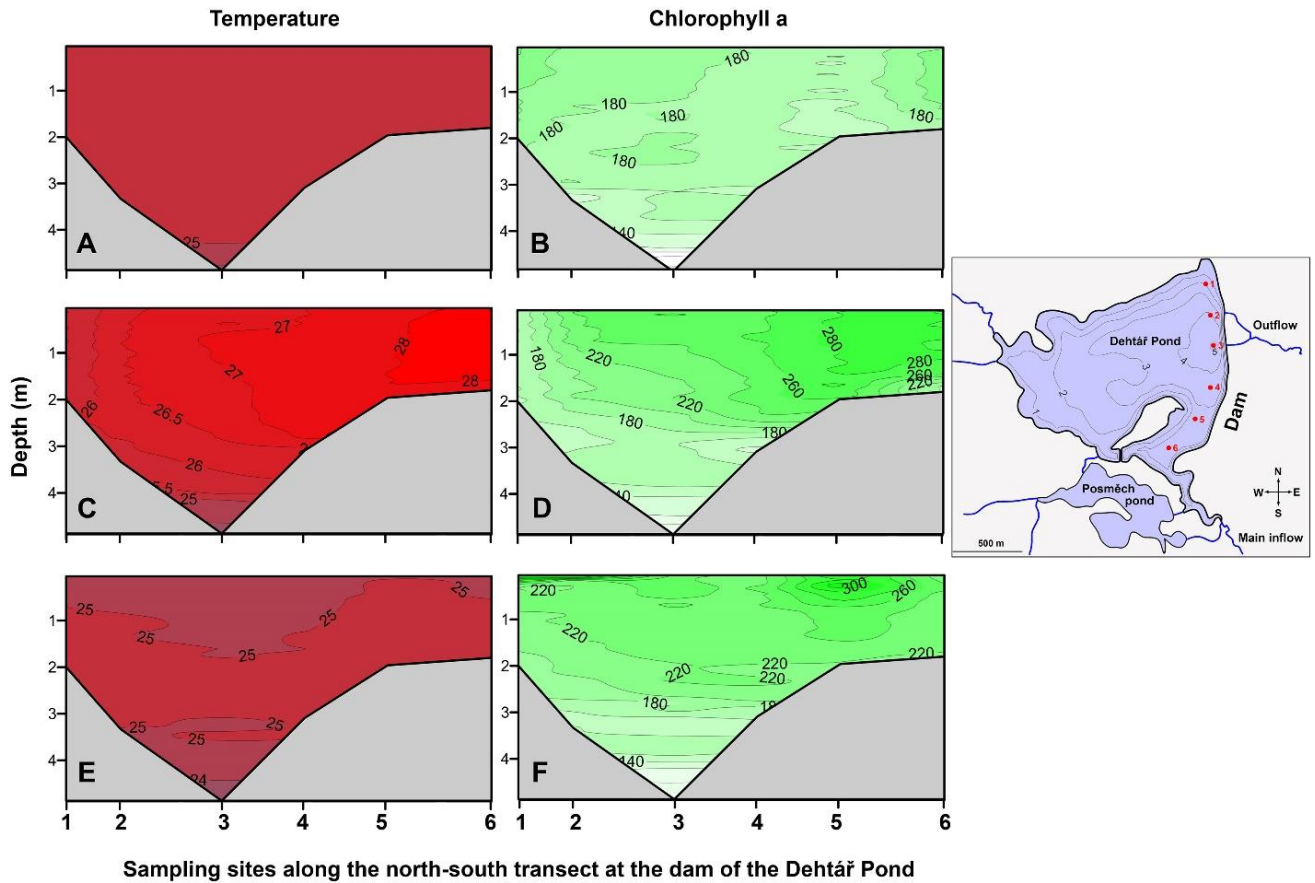
Figure S5. Contour graphs illustrating both seasonal and daily changes in spatial heterogeneity (indicated by the coefficient of variation, CV%) of the surface water temperature (°C) in the fishpond.
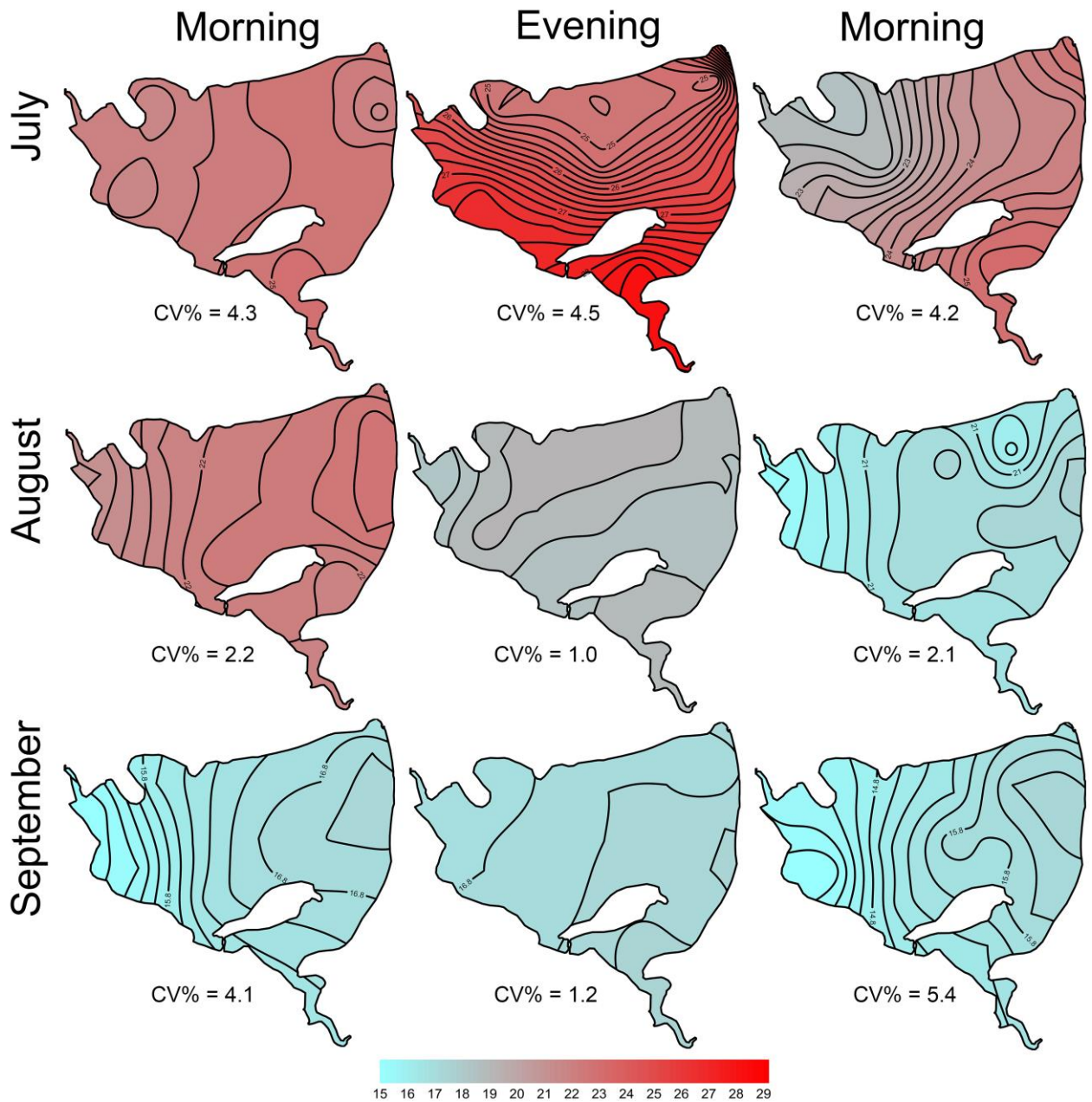
Figure S6. Contour graphs illustrating both seasonal and daily changes in spatial heterogeneity (indicated by the coefficient of variation, CV%) of the surface pH in the fishpond.
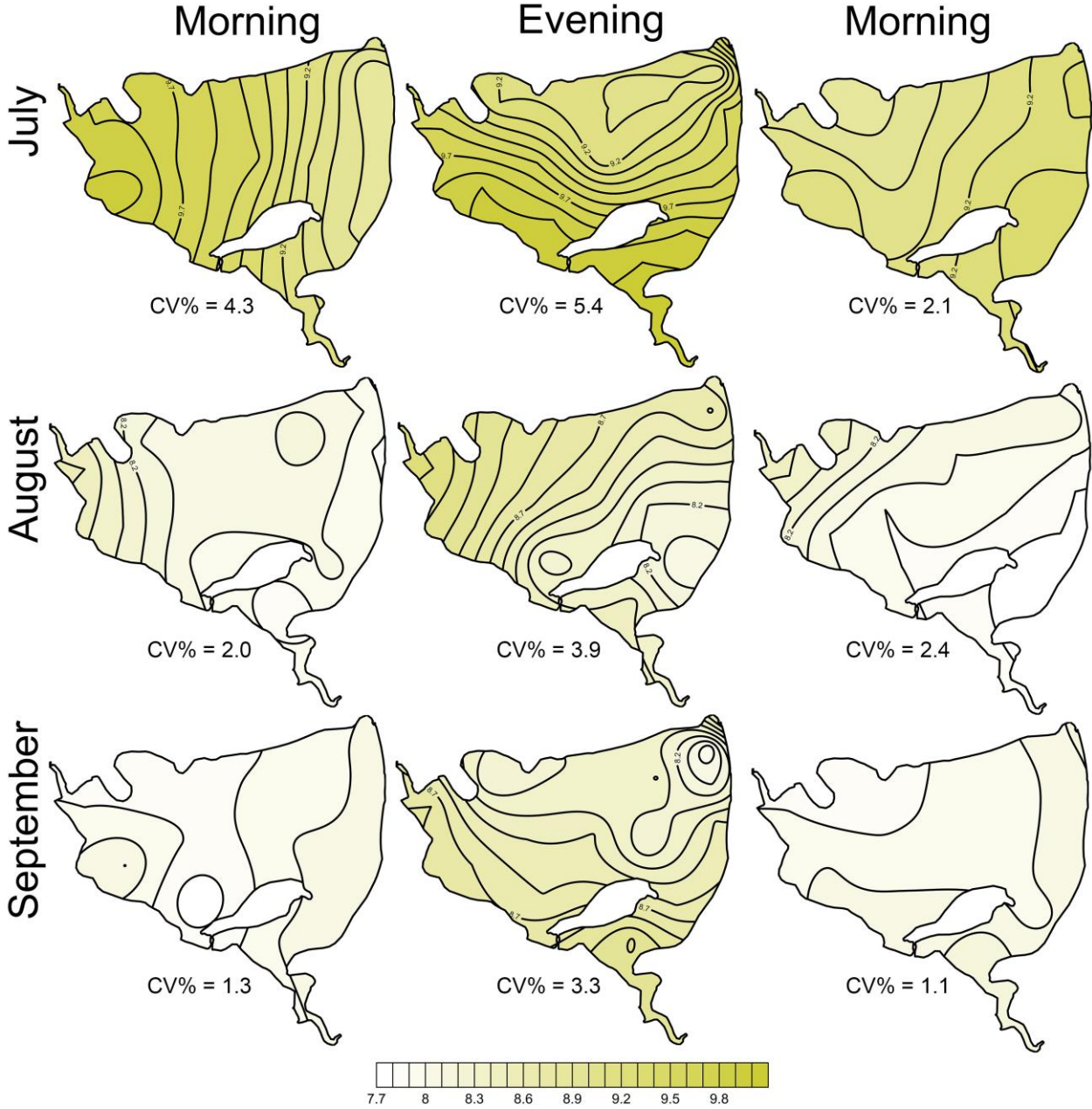
Figure S7. Contour graphs illustrating both seasonal and daily changes in spatial heterogeneity (indicated by the coefficient of variation, CV%) of the surface oxygen concentration (mg L^{-1}) in the fishpond.
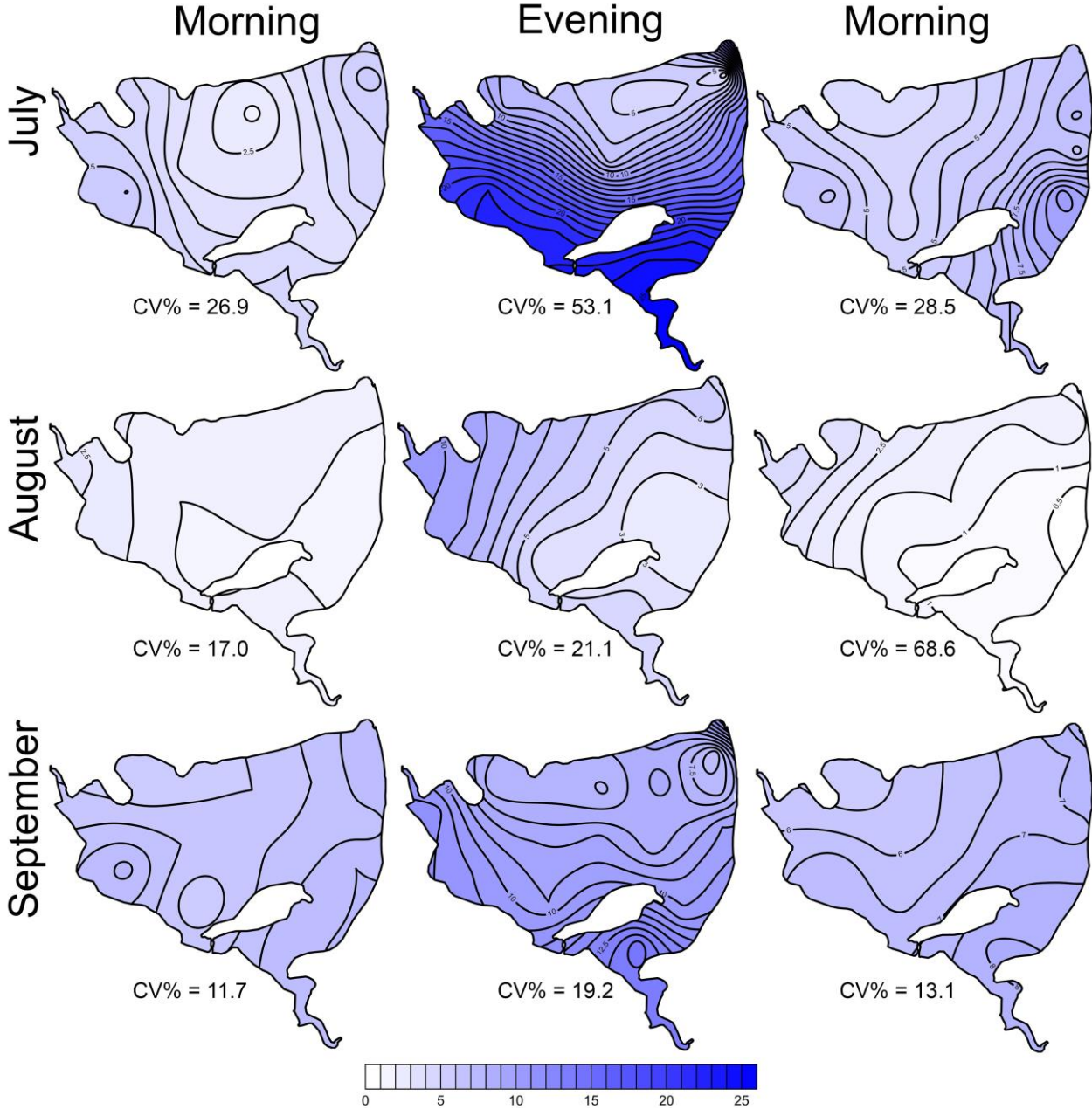
Figure S8. Contour graphs illustrating both seasonal and daily changes in spatial heterogeneity (indicated by the coefficient of variation, CV%) of the surface chlorophyll-a concentration ($\mu g\ L^{-1}$) in the fishpond.
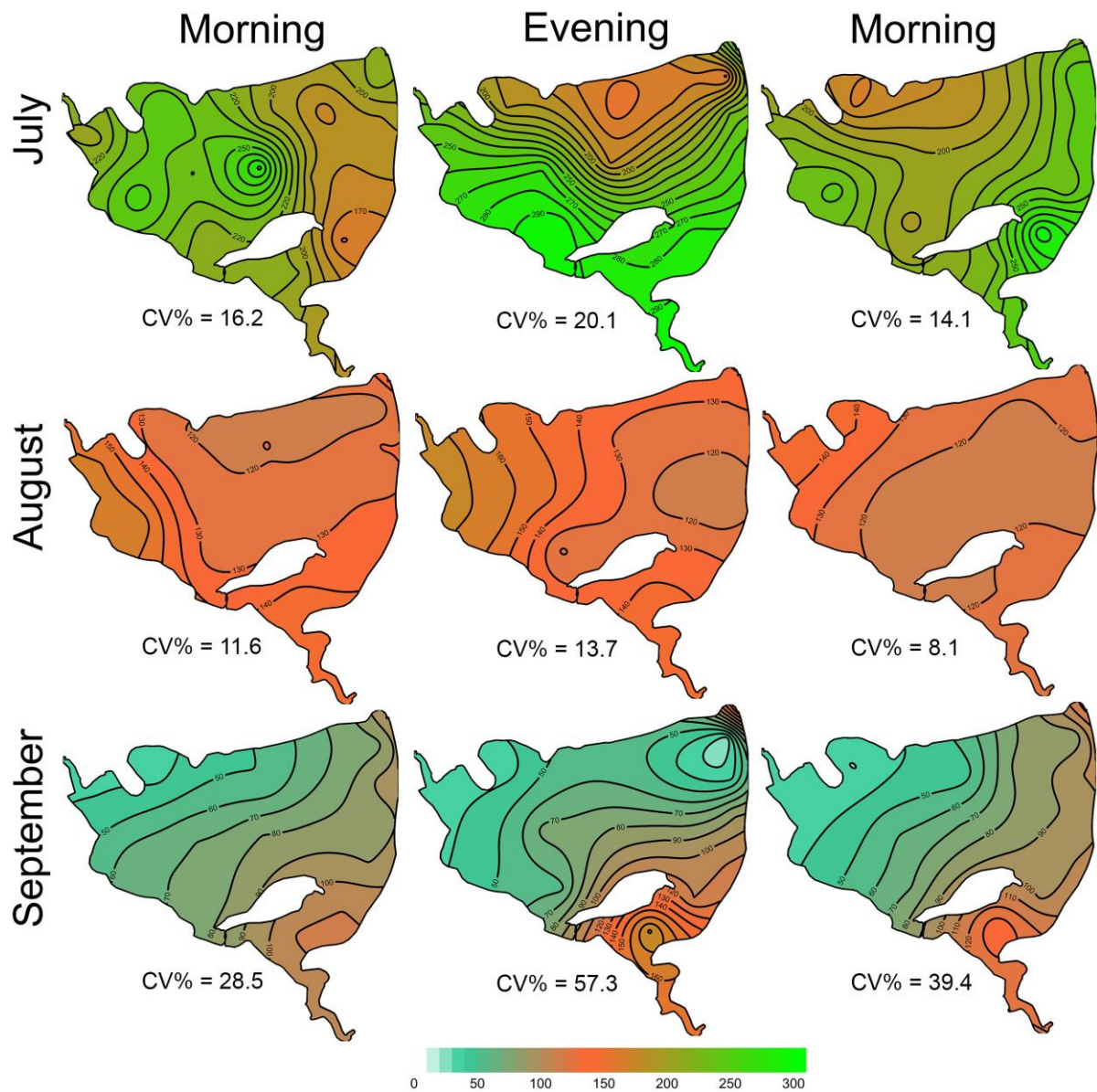
Figure S9. Daily course of wind speed during July measurement. Arrows indicate sampling times.
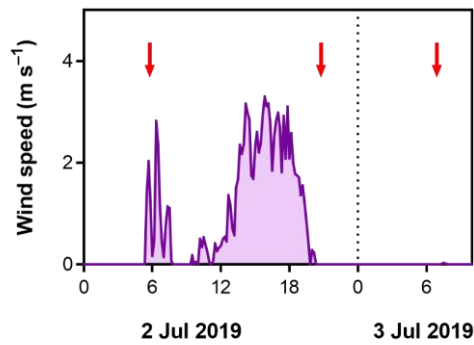

Figure S10. Conceptual diagram of the effects of wind on spatial heterogeneity in the pond. The unidirectional wind blowing along the north-south axis of the pond resulted in the lateral movement of surface water to the south, which in turn initiated the whole-lake circulation and the upwelling of colder and oxygen-depleted water in the north (indicated by arrows). After several hours of the wind disturbance, pronounced north-south gradients of temperature, oxygen and chlorophyll-a built up, as indicated by the horizontal triangle and colours. The vertical triangle depicts the vertical structure of the water column before the wind event.
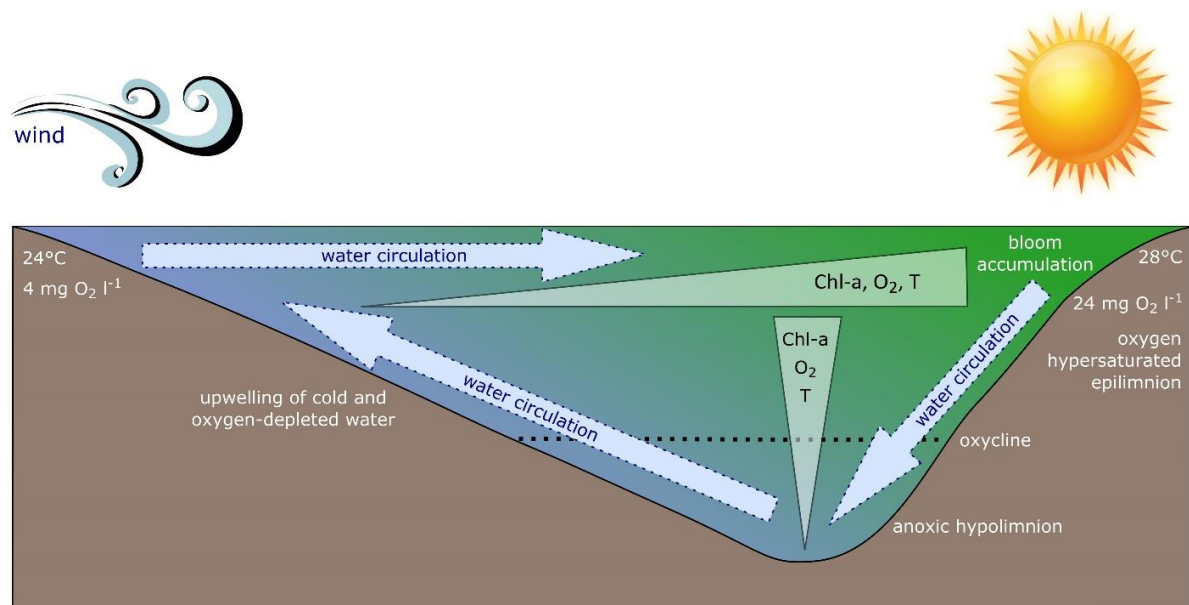
Figure S11. Violin plot of the surface methane concentration in water during the season. Solid lines are medians; dashed lines denote quartiles. Asterisks indicate significant differences (*** $p < 0.001$, **** $p < 0.0001$) between sampling dates determined by two-way ANOVA with Tukey's multiple comparison test.
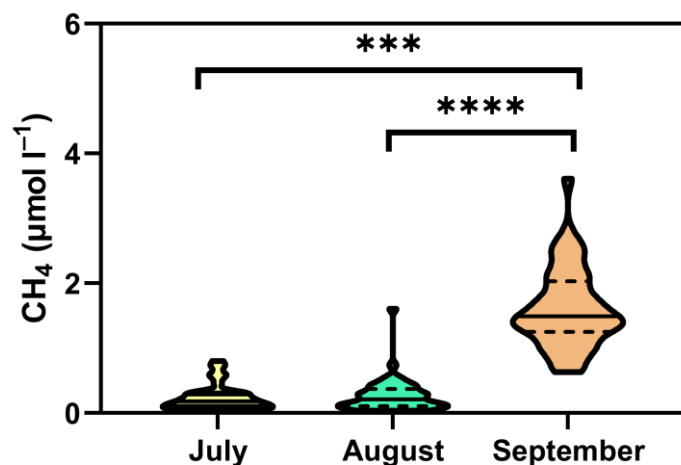
Figure S12. Whole-system estimates of the methane efflux from the pond. We estimated the total efflux using the average spatially pooled CH_4 flux (WSAvg) in every campaign and then multiplied it by the fishpond surface area. To demonstrate the bias introduced from a single point measurement, we did the same for the deepest point (Site 3), usually representing the system in standard monitoring programs. Numbers are daily methane efflux in kg.

Figure S13. Diurnal changes of oxygen measured in the first campaign in July, where the diurnal variation was highest.

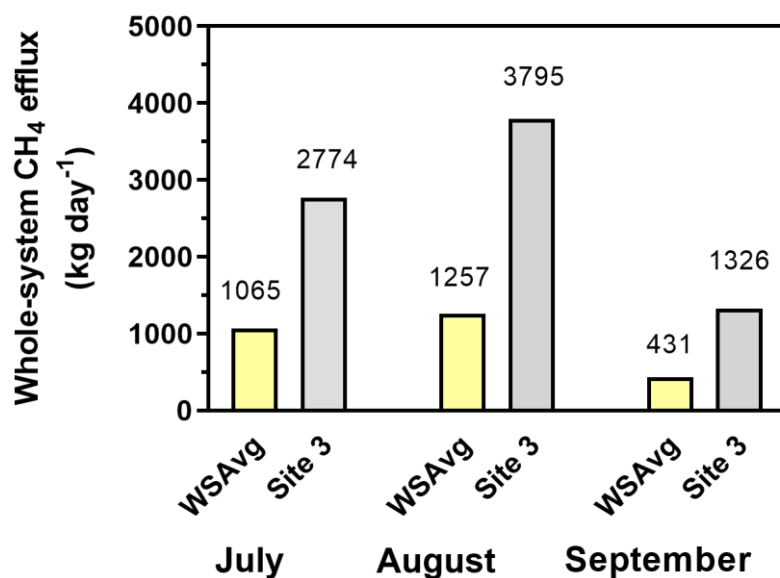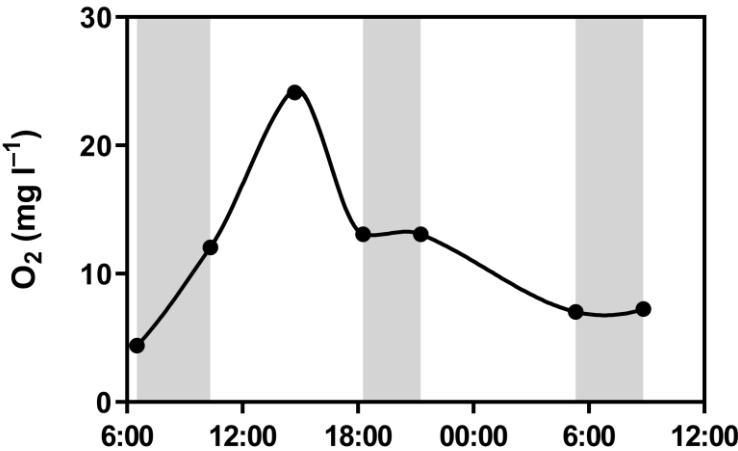**Table S1.** A summary of spatial gradients calculated with linear regression using geographic coordinates of sampling sites. West-east (W-E, "longitudinal") gradient is identical to the direction from the shallowest part of the pond (e.g. Site 15) towards the dam (e.g. Site 5), while the south-north (S-N, "lateral") gradient goes along to the dam. Geographic coordinates were recalculated to km and expressed as the distance from the most western (15) and southernmost (6) sites. Parameter values were normalized, calculating per cent of the average of all 15 sites and gradients (slopes) were expressed in the units of %/km. Positive values mean increasing, negative decreasing values of respective parameters along to W-E or S-N axis. Where slopes did not differ significantly from zero ($p > 0.05$, F-test), gradients were considered non-existent. We also evaluated the stability of temporal gradients (changes in gradients between consecutive samplings, i.e. morning-evening, evening-next morning), comparing differences in respective slopes with F-test. Generally, W-E gradients ("longitudinal", along the depth gradient) were confirmed much more frequently (28 of 54 cases) and in all sampling campaigns and daytimes. In comparison, the S->N gradients occurred less frequently (11 of 54 cases) and mainly in July and September in the evening. Spatial trends in limnological parameters were common, while trends in methane fluxes were scarce: no trend in CH_4 diffusive fluxes was detected. Longitudinal gradients came up mostly overnight, likely due to uneven changes in fishpond metabolism, while the lateral gradients were formed likely in response to the wind.

Gradient direction	Month	Variable	Gradient M1 %/km	Gradient E1 %/km	Gradient M2 %/km	Changes in gradient (F-test) M1→E1 P	Changes in gradient (F-test) E1→M2 P
S→N	Jul	CH4-diff	*none*	*none*	*none*	*n.s.*	*n.s.*
		CH4-tot	n.d.	*none*	*none*	n.d.	*n.s.*
		pH	*none*	**-11.4**	*none*	*n.s.*	0.0011
		Tw	*none*	**-10.76**	*none*	0.0035	0.0114
		O2	*none*	**-130**	*none*	<0.0001	0.0003
		Chla	*none*	**-47.3**	**-8.31**	0.0069	0.0086
	Aug	CH4-diff	*none*	*none*	*none*	*n.s.*	*n.s.*
		CH4-tot	n.d.	*none*	*none*	n.d.	*n.s.*
		pH	*none*	*none*	*none*	*n.s.*	*n.s.*
		Tw	*none*	*none*	*none*	*n.s.*	*n.s.*
		O2	*none*	*none*	*none*	*n.s.*	*n.s.*
		Chla	**-16.5**	*none*	**2.13**	*n.s.*	*n.s.*
	Sep	CH4-diff	*none*	*none*	*none*	*n.s.*	*n.s.*
		CH4-tot	n.d.	*none*	*none*	n.d.	*n.s.*
		pH	*none*	**-7.43**	*none*	0.0002	0.0004
		Tw	*none*	*none*	*none*	*n.s.*	*n.s.*
		O2	*none*	**-42.2**	*none*	0.005	0.0207
		Chla	*none*	**-110**	**-27.5**	0.0417	*n.s.*
W→E	Jul	CH4-diff	*none*	*none*	*none*	*n.s.*	*n.s.*
		CH4-tot	n.d.	**109**	**99.5**	n.d.	*n.s.*
		pH	**-6.78**	**-6.254**	**2.35**	*n.s.*	<0.0001
		Tw	**6.41**	*none*	**6.02**	0.0049	0.0085
		O2	*none*	*none*	**28.6**	*n.s.*	*n.s.*
		Chla	**-16.1**	*none*	**11.6**	*n.s.*	*n.s.*
	Aug	CH4-diff	*none*	*none*	*none*	*n.s.*	*n.s.*
		CH4-tot	n.d.	*none*	**129**	n.d.	*n.s.*
		pH	**-2.55**	**-4.837**	**-2.69**	*n.s.*	*n.s.*

		Tw	**2.92**	*none*	**2.55**	0.0012	0.0116
		O2	*none*	**-69.4**	**-85.5**	0.0006	n.s.
		Chla	*none*	**-18.3**	**-7.2**	*n.s.*	0.026
	Sep	CH4-diff	*none*	*none*	*none*	*n.s.*	*n.s.*
		CH4-tot	n.d.	*none*	*none*	n.d.	*n.s.*
		pH	*none*	*none*	**1.1**	*n.s.*	*n.s.*
		Tw	**6.07**	**1.53**	**8.34**	<0.0001	<0.0001
		O2	**10.6**	*none*	**16.2**	*n.s.*	0.0355
		Chla	**35.2**	*none*	**-27.5**	*n.s.*	*n.s.*